

Elastic Buckling Loads of Fixed Frames By The Newmark Method

A. Badir

Department of Environmental & Civil Engineering, U.A. Whitaker College of Engineering, Florida Gulf Coast University, Florida, US,

ABSTRACT: A numerical method for the solution of the elastic stability of fixed frames is presented. The Newmark iterative procedure to perform elastic buckling analyses for isolated columns is extended for use in computing buckling loads and buckling modes in frames with fixed columns. The method is illustrated in details by means of different cases of single-storey portal frames commonly used in commercial buildings. Comparisons of obtained results with other well known methods show very good agreement.

KEYWORDS: Numerical Analysis; Elastic Stability; Buckling; Critical Load; Fixed Frames.

1 INTRODUCTION

The elastic critical load of a bar with uniform or non-uniform cross section can be calculated by a numerical method of double integration (Newmark 1943). Instead of assuming the deflection y as some function of x , the beam is divided into segments and a numerical value of deflection is assumed at each division point along the beam. The subsequent calculations are made, determining ordinates to the M/EI diagram (M is the moment, E is the elastic modulus of the material and I is the area moment of inertia), and new values of deflections at each site. If these are equal to the assumed deflections at every division point, then the required critical load P and the buckling mode are determined. If they are not equal, the new set of deflections is assumed and the calculations are repeated. This procedure is successful because the results of each cycle yield better deflections and the procedure converges to the exact buckling mode after a few numbers of cycles of iteration.

The technique of Newmark's numerical method (Newmark 1943), applied to columns, has been extended for use in computing buckling loads and buckling modes of hinged frames (Badir 2011). In this paper, Newmark's method is further extended for the case of frames with fixed columns. The analysis and results are reported herein with detailed calculations in order to illustrate the method for two cases; namely, (1) rigidly jointed elastic portal frames with fixed columns without sway, as in symmetrical modes or when translation of the joints is prevented for, and (2) rigidly jointed elastic frames with fixed columns, with sway as in anti-symmetrical modes.

The philosophy of the method described herein can be summarized as follows: the buckling load of the structure is the load just enough to maintain it in an

assumed buckling configuration. The method involves cycles of iteration in which a new configuration better than the assumed one is obtained at the end of each cycle. The calculations can be repeated until the required degree of accuracy is obtained. In most cases, accurate results are obtained after only few cycles.

2 SYMMETRICAL MODE OF BUCKLING OF FIXED FRAMES

Consider the fixed frame shown in Fig. 1, the end forces and rotations of each member are separately shown in Fig. 2. The column AB is subjected to three forces at B, namely: vertical force P , end couple X_1 , and horizontal force X_2 . The end rotations φ at B or C can be easily determined from the horizontal beam BC: $\varphi = (L_b/2EI_b) X_1$, neglecting the effect of axial force X_2 .

Our goal is to determine P , X_1 , and X_2 which are just enough to maintain the structure in its assumed buckling shape (y_a) and satisfy the end conditions at B, namely:

1. Rotation φ at B of both column BA and beam BC is equal to $(L_b/2EI_b) X_1$.
2. Horizontal displacement at B equal zero.

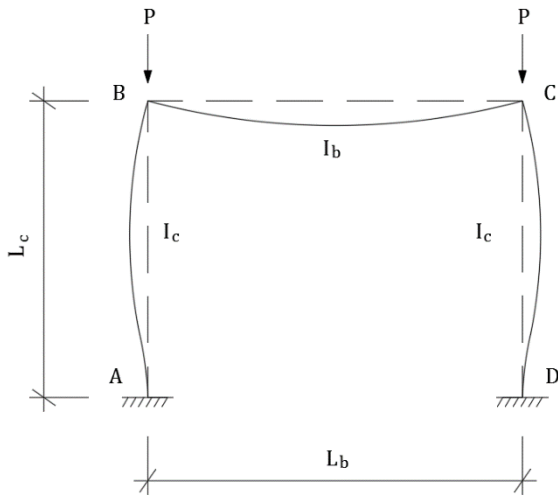


Figure 1 Symmetrical Fixed Frame

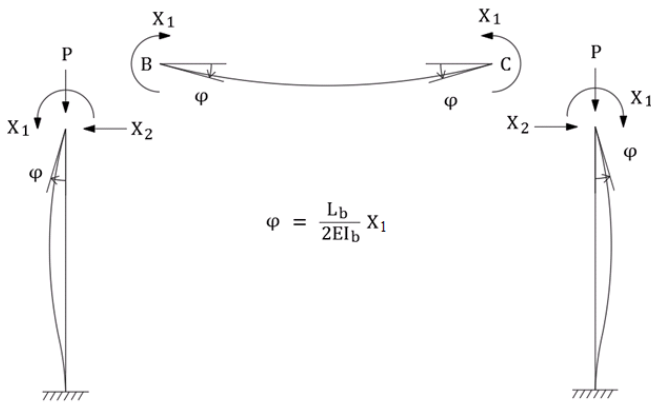


Figure 2 Symmetrical fixed frame: end forces and rotations

Figure 3(a) shows the column AB and the end forces at B, the column under these forces can be regarded as the superposition of Fig. 3(b), Fig. 3(c) multiplied by X_1 , and Fig. 3(d) multiplied by X_2 . Hence

$$\varphi_p + X_1\varphi_{x_1=1} + X_2\varphi_{x_2=1} = \frac{L_b}{2EI_b} X_1 \quad (1)$$

$$y_p + X_1y_{x_1=1} + X_2y_{x_2=1} = 0 \quad (2)$$

Figure 4 shows the calculations of the last cycle of the frame shown in Fig. 1. Line 1 in Fig. 4 represents the assumed set of deflections obtained from the previous cycle where the fixed column AB is divided into seven sections (6 segments), each segment of length equal to λ . The assumed set of deflection y_a of the first cycle, not shown in Figure 4, represents a sine curve of amplitude 1000 at the middle of the column. The final result does not depend on the starting assumed function, the method converges to the correct buckling mode after a few

number of cycles. Normal calculations (Newmark 1943) are recorded from line 2 to line 18 as follows

Line 2 corresponding values of angle changes α ($\alpha = M/EIc$) commonly known as the elastic load. A common factor is shown at the end of each line, for line 2 the common factor is P/EIc

Line 3 equivalent concentrated elastic load $\bar{\alpha}$ acting on each section. The values of these concentrations are computed with sufficient accuracy from the formulae given in the work of Newmark (1943).

Lines 4 and 5 The shearing forces and bending moments in the conjugate beam are calculated from the concentrated loads $\bar{\alpha}$ (in line 3). They represent the average slopes φ , and the deflections y_p , respectively.

Line 6 the slope at B, due to the axial load P is thus found to be $\varphi_p = (3368 + 104)P\lambda/EI_c = 3472 P\lambda/EI_c$.

The fixed ended column AB is then subjected to a unit couple, $X_1 = 1$, at its end B. Normal calculations are shown from line 7 to 9. In line 10 are given the values of average slope φ_{av} in the different segments. In line 11 the deflections are obtained starting with zero value at the fixed end. The resulting deflection at B has a value of $-18\lambda^2/EI_c$.

Line 12 slope at B due to a unit couple, $\varphi_{x_1=1}$ is equal to $(-5.5 - 0.5)\lambda/EI_c = -6\lambda/EI_c$

Lines 13 through 18 corresponds to the case of Fig. 3(d).

The following variables of Eqs. (1) and (2) are determined:

$$\varphi_p = 3472 P\lambda/EI_c \text{ (from line 6),}$$

$$y_p = 9157 P\lambda^2/EI_c \text{ (from line 5),}$$

$$\varphi_{x_1=1} = -6.0\lambda / EI_c \text{ (from line 12),}$$

$$y_{x_1=1} = -18.0\lambda^2 / EI_c \text{ (from line 11),}$$

$$\varphi_{x_2=1} = -18.0\lambda^2 / EI_c \text{ (from line 18), and}$$

$$y_{x_2=1} = -72.0\lambda^2 / EI_c \text{ (from line 17).}$$

By solving these equations for a stiffness ratio $K_c/K_b = 1$, where $K_c = EI_c/L_c$, $K_b = EI_b/L_b$, and noticing that $L_c = 6\lambda$, we get $X_1 = +262.83 P$ and $X_2 = 61.472 P/\lambda$

Line 19 same as line 5

Line 20 line 11 multiplied by X_1

Line 21 line 17 multiplied by X_2

Line 22 superposition of the three previous lines

Line 23 line 1 divided by line 22 giving the ratio y_a/y at every division point which appears to be almost the same.

The critical load calculated from the better ratio $\Sigma y_a/\Sigma y$ is $0.70186 EI_c/P\lambda^2$ for the case of stiffness ratio $K_c / K_b = 1$, giving a critical load with a value of $25.267 EI_c / L_c^2$, which is the same as the value of

25.266 $EI_c / L^2 c$ given by Horne and Merchant (1965). The assumed buckling mode of a next cycle, see last line of Fig. 4, is almost identical to the previous one. One may notice that line 7 to line 18 are

unaltered, hence they are only calculated in the first cycle.

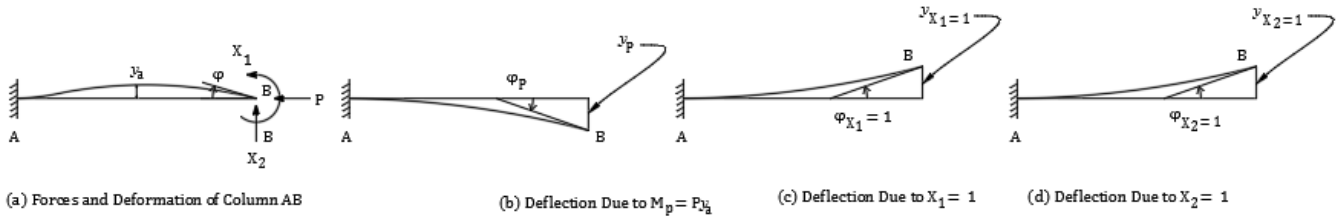


Figure 3 Symmetrical fixed frame: superposition, Fig. 16(a) = Fig. 16 (b) + X_1 Fig. 16 (c) + X_2 Fig. 16 (d)

1- y_a	0	-200	-640	-1000	-990	-580	0		
2- α		200	640	1000	990	580	0	P/EIc	
3- $\bar{\alpha}$	23	220	633	969	952	566	104	$P\lambda/EIc$	
4- φ		23	243	876	1845	2802	3368	$P\lambda/EIc$	
5- y_p	0	23	266	1142	2987	5789	9157	$P\lambda^2/EIc$	
6- φ_p							3472	$P\lambda/EIc$	
7- M	1	1	1	1	1	1	1		
8- α	-1	-1	-1	-1	-1	-1	-1	1/EIc	
9- $\bar{\alpha}$	-0.5	-1	-1	-1	-1	-1	-0.5	λ/EIc	
10- φ_{av}		-0.5	1.5	-2.5	-3.5	-4.5	-5.5	λ/EIc	
11- $y_{x_1=1}$	0	-0.5	-2.0	-4.5	-8.0	-12.5	-18	λ^2/EIc	
12- $\varphi_{x_1=1}$							-6	λ/EIc	
13- M	6	5	4	3	2	1	0	λ	
14- α	-6	-5	-4	-3	-2	-1	0	λ/EIc	
15- $\bar{\alpha}$	-2.83	-5	-4	-3	-2	-1	-0.16	λ^2/EIc	
16- φ_{av}		-2.83	-7.83	-11.83	-14.83	-16.83	-17.83	λ^2/EIc	
17- $y_{x_2=1}$	0	-2.83	-10.66	-22.5	-37.33	-54.16	-72	λ^3/EIc	
18- $\varphi_{x_2=1}$							-18	λ^2/EIc	
19- y_p	0	23	266	1142	2987	5789	9157	$P\lambda^2/EIc$	
20- $X_1 y_{x_1=1}$	0	-131.42	-525.66	-1182.74	-2102.64	-3285.32	-4731	$P\lambda^2/EIc$	
21- $X_2 y_{x_2=1}$	0	-174.17	-655.70	-1383.13	-2294.96	-3329.75	-4426	$P\lambda^2/EIc$	
22- y	0	-282.59	-915.36	-1423.87	-1410.60	-826.13	0	$P\lambda^2/EIc$	
23- y_a/y		0.7077	0.6992	0.7023	0.7018	0.7021		$EIc/P\lambda^2$	

Better Ratio = $(3410/4858.55) EIc/P\lambda^2 = 0.70186 EIc/P\lambda^2$

Critical Load $P_{cr} = 0.70186 \times 36 EIc/L^2 c = 25.267 EIc/L^2 c$

Assumed Buckling Mode of Next Cycle :

y_a	0	-198	-643	-1000	-990	-580	0
-------	---	------	------	-------	------	------	---

Figure 4 Calculation of critical load P_{cr} for symmetrical fixed frame (last cycle)

3 ANTISYMMETRICAL MODE OF BUCKLING OF FIXED FRAMES

Consider the single-bay fixed frame shown in Fig. 5 with antisymmetrical mode of buckling.

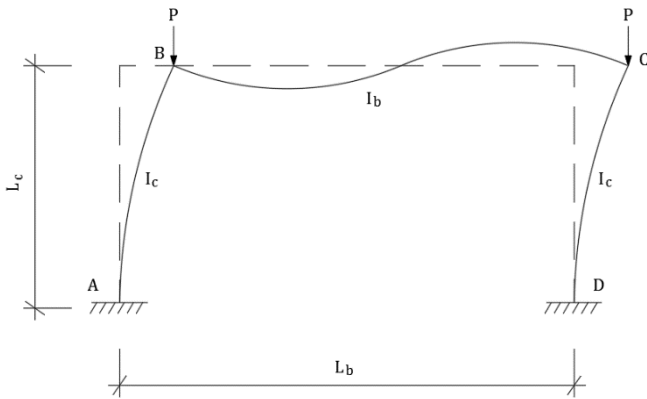


Figure 5 Antisymmetrical fixed frame

The end forces and rotations for each member are separately shown in Fig. 6.

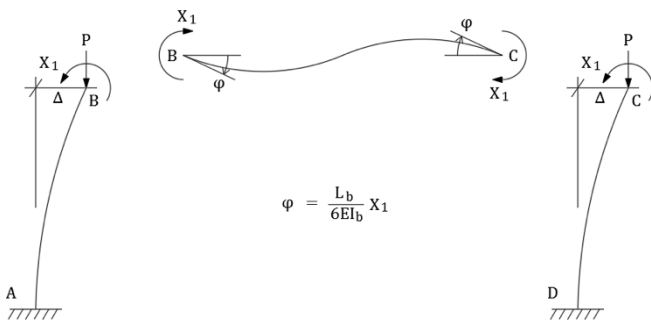


Figure 6 Antisymmetric fixed frame: end forces and rotations

The column AB is subjected to only two forces at B, namely: vertical force P and a couple X_1 . The end rotation ϕ at B or C is equal to $(L_b/6EI_b) X_1$. Figure 7 shows the column AB with an arbitrary sideways of $\Delta = 1000$ units at B. The columns can be regarded to as the superposition of Fig. 7(b) and Fig. 7(c) multiplied by X_1 . Hence

$$\phi = \phi_p + X_1\phi_{x_1=1} = \frac{L_b}{6EI_b} X_1 \quad (3)$$

$$y = y_p + X_1y_{x_1=1} \quad (4)$$

Where ϕ_p and y_p are the rotation and deflection at B due to the axial force P , $\phi_{x_1=1}$ and $y_{x_1=1}$ are the rotation and deflection at B due to unit couple acting at B. From Eq. (3) X_1 is determined and then y is calculated from Eq. (4). Figure 8 shows complete calculations of the last cycle, in which column AB is assumed to buckle in the shape reached at this cycle. The assumed set of deflection y_a of the first cycle, not shown in Fig. 8, represents a straight line varying from a value of zero at A to a value of 1000 at B. However, the final result does not depend on the starting deflection assumption. The better ratio $\Sigma y_a / \Sigma y$ is $0.20518EI_c / P\lambda^2$ for the case of stiffness ratio $K_c / K_b = 1$, giving a critical load with a value of $7.386EI_c / L_c^2$. The same problem was solved by Horne and Merchant (1965) and a value of $7.378EI_c / L_c^2$ was obtained.

4 CONCLUSIONS

The Newmark's double integration procedure is extended for use in computing critical loads and buckling modes of rigidly jointed frames with fixed columns. Results obtained show very good agreement with well-known methods. The elastic line of the mode of buckling is determined as a major part of the solution, which gives a clear insight of the behavior of the structure. The method presented here can be used to study buckling of frames with varying cross sections.

5 REFERENCES

- Badir, Ashraf, (2011). "Elastic Buckling Loads of Hinged Frames by the Newmark Method," *International Journal of Applied Science and Technology*, Vol. 1 No 3.
- Horne, M. R., and Merchant, W., (1965). "The stability of frames," *Pergamon*, Oxford.
- Newmark, N. M., (1943). "Numerical procedure for computing deflections, moments, and buckling loads," *Trans. ASCE*, vol. 108, Paper No. 2202, pp. 1161-1188.

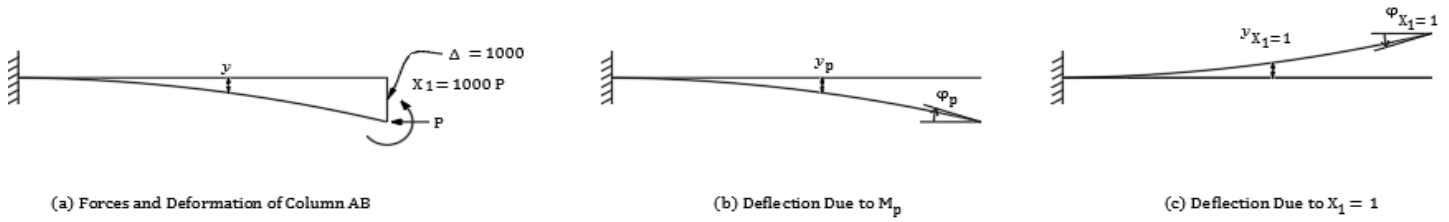


Figure 7 Antisymmetrical fixed frame: superposition, Fig. 20(a) = Fig. 20 (b) + X₁ Fig. 20 (c)

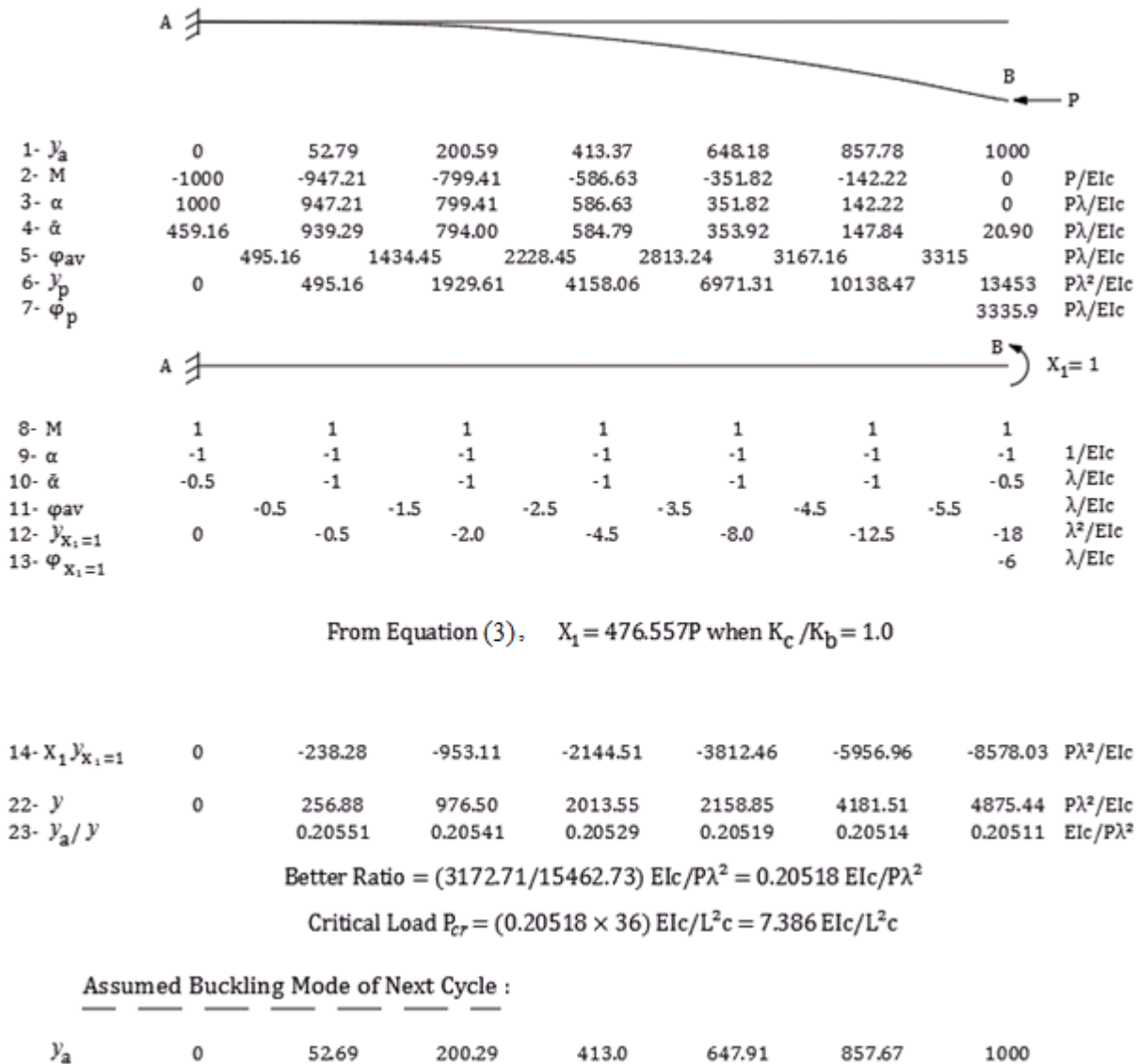


Figure 8 Calculation of critical load Pcr for antisymmetrical fixed frame (last cycle)